Environ Geochem Health (2023) 45:4057–4069
https://doi.org/10.1007/s10653-022-01436-0

CORRESPONDENCE

The spatial analysis, risk assessment and source identification for mercury in a typical area with multiple pollution sources in southern China

Zhaohui Feng · Li Deng · Yikai Guo · Guanghui Guo · Lingqing Wang · Guangjin Zhou · Yizhong Huan · Tao Liang

Received: 8 October 2022 / Accepted: 11 November 2022 / Published online: 7 December 2022
© The Author(s), under exclusive licence to Springer Nature B.V. 2022

Abstract Mercury (Hg) has always been a research hot spot because of its high toxicity. This study conducted in farmland near rare earth mining area and traffic facilities, which considered multiple pollution sources innovatively. It not only analyzed Hg spatial characteristics using inverse distance weighting and self-organizing map (SOM), but also assessed its pollution risk by potential ecological risk index (Er) as well as geoaccumulation index (I_{geo}), and identified the pollution sources with positive matrix factorization. The results showed that there was no heavy Hg pollution in most farmland, while a few sampling sites with Hg pollution were close to highway, railway station and petrol station in Xinfeng or in the farmland of Anyuan, which were divided into the cluster with highest Hg concentration in SOM. The vehicle exhaust emission and pesticide as well as fertilizer additions significantly contributed to the local Hg pollution. Besides, there was moderate pollution and high ecological risk in Anyuan assessed by I_{geo} and Er, respectively. In contrast, Xinfeng had the moderate and considerable ecological risks in a larger scale. The enriched Hg might harmed not only the nearby ecological environment, but also the human health when it entered human body through food chain. The three factors that contributed to mercury concentration in this area according to positive matrix factorization were natural source, traffic source and agricultural source, respectively. This study about Hg pollution in the typical area would provide scientific evidence for the particular treatment of Hg pollution from various pollution sources like traffic source, agricultural source, etc.

Keywords Mercury pollution · Risk assessment · Source identification · Positive matrix factorization · Self-organizing map

Supplementary Information The online version contains supplementary material available at https://doi.org/10.1007/s10653-022-01436-0.

Z. Feng · G. Guo · L. Wang (✉) · G. Zhou · T. Liang
Key Laboratory of Land Surface Pattern and Simulation, Institute of Geographic Sciences and Natural Resources Research, Chinese Academy of Sciences, Beijing 100101, China
e-mail: wanglq@igsnrr.ac.cn

Z. Feng
University of Chinese Academy of Sciences, Beijing 100049, China

L. Deng · Y. Guo
Ecological Environment Planning and Environmental Protection Technology Center of Qinghai Province, Xining 810007, China

Y. Huan
School of Public Policy and Management, Tsinghua University, Beijing 100084, China

Introduction

As one of the most toxic heavy metals in the natural world, mercury (Hg) with the high toxicity and migration has brought wide attention (Campos et al., 2018; Shahid et al., 2020; Zhou et al., 2018). Harm from Hg even occurs in the long distance from its initial source because of the long-distance transport, which expands its distributing range in air, water or soil (Lawrence et al., 2013; Tang et al., 2020). The World Health Organization pointed out that Hg was harmful for the skin, eye, lung, kidney and other organs as well as the digestive, immune and nervous systems. It is recognized as one of the ten harmful substances causing the serious public health problem (WHO, 2019). Except for the direct contact, the consumption of plants containing mercury also threats human health (Shahid et al., 2020). Therefore, it is important to analyze the spatial distribution of Hg and trace its potential risk sources.

Mercury can be normally decomposed and released from rock or soil under the functions of water, wind or volcanic activities in natural state. In addition, it also comes from human activities (Shahid et al., 2020). Previous studies reported that some mining activities lead to Hg contaminant in water or soil, which polluted the adjacent ecosystem (Beckers et al., 2019; Osterwalder et al., 2019). Moreover, the dust generated by vehicle exhaust due to the Hg addicted fuel made the Hg disperse near roads or other traffic facilities with the increase in traffic, which has become an important source of soil Hg pollution and exerts negative impacts on nearby ecological environment (Chary et al. 2008; Liu et al., 2012). Besides, the impact on the Hg in grain from mercury-containing pesticides had also become the research focus, the rice consumption brought high organic Hg exposure risks indirectly because Hg entered human body via food chain (Jiang et al., 2021; Wang et al., 2021; Yeganeh et al., 2013). It can be concluded that the agricultural additions of pesticides and fertilizers, as the important external inputs of Hg, should be given enough attention.

Self-organizing map (SOM) belongs to the unsupervised machine learning method and has superior performance in processing nonlinear problem (Mari et al., 2010). As a classic competitive neural network, SOM produced the best matching units and acquired good classifying and visualizing results for input samples. It has already applied for pattern recognition of heavy metals and pollutants in water or soil (Wang et al., 2020). Geoaccumulation index (I_{geo}) for evaluating heavy metal contamination can explicit Hg contamination and its distribution heterogeneity effectively and vividly (Bing et al., 2011). The risk assessment for Hg by potential ecological risk index (*Er*) is helpful for the prediction of subsequent ecological risk and reflects the ecological impact of Hg content under certain environment through combining the toxicological, environmental and ecological effects (Antoniadis et al., 2019; Tabassum et al., 2019; Wang et al., 2020). Besides, positive matrix factorization (PMF) is a classic model for source identification, which is used for the source apportion of pollutants in soil, air and sediment popularly (Lv et al., 2019; Magesh et al., 2021). The environmental parameters for the transfer or dispersion of pollutant as well as the pollutant emission inventory are not necessary for PMF, which avoids the deviations resulted from the meteorological or topographical factors effectively (Taghvaee et al., 2018).

Ganzhou City in Jiangxi Province is not only rich in rare earth resources, but also an important transportation hub connecting four provinces in Southeast China (Cheng, 2009; Yang et al., 2013). The research area located in the south of Ganzhou is adjacent to the mining area as well as traffic facilities, and it has developed agriculture, which probably increased the potential pollution of Hg (Xue et al., 2013). Most previous studies paid attention to the potential pollution of toxic elements in mining areas, while this study about Hg pollution considered multiple pollution sources including traffic, mining and smelting as well as farming activities in a typical area innovatively. Combining with various influencing factors, this study aims to: (i) analyze the spatial distribution of Hg and classify the Hg concentrations; (ii) assess the Hg pollution risk; and (iii) identify the pollution sources of Hg in a typical area in Jiangxi Province. This study will give the better comprehension of Hg pollution and its subsequent health risk in a typical area with several possible pollution sources.

Material and methods

Study area

The typical area for this research (114° 34′ 27″ E–115° 30′ 55″ E, 24° 51′ 56″ N–25° 32′ 30″ N) is in Ganzhou City in the south of Jiangxi Province, China, which is mainly in two counties—Xinfeng and Anyuan as shown in Fig. 1. This typical area is adjacent to mining area and traffic facilities. Part of it in Xinfeng was mainly planted with rice, and part of it in Anyuan was mainly planted with fruit trees. The altitude of the study area ranges from 109 to 1152 m, and there is mainly red soil. This typical region belongs to subtropical monsoon climate, with hot summer and warm winter as well as four distinct seasons. There is also simultaneous rain and heat, and developed monsoon in summer (Yu et al., 2020). Its subtropical climate is suitable for the plantation of subtropical crops, especially the rice and orange. Besides, Ganzhou with superior geographical location has become an important transportation hub, which connects many essential economic regions of China. The south region of Ganzhou with rich rare earth reserves has formed developed industries and significantly contributed to local economic development (Zhao et al., 2019). Of course, the relative resource mining has put heavy burden on local ecological environment in many areas such as Anyuan County as previous study reported (Li et al., 2020).

Soil sampling and analysis

This study collected 78 surface soil samples (0–20 cm) in Xinfeng (46 soil samples) and Anyuan (32 soil samples) in the south part of Ganzhou, and their geographical positions are in Fig. 1. The systematic random distribution method was adopted when the sample positions were determined. The actual geographical sites for sampling were adjusted according to the local environment in the south of Ganzhou. The soil samples were collected and saved in plastic

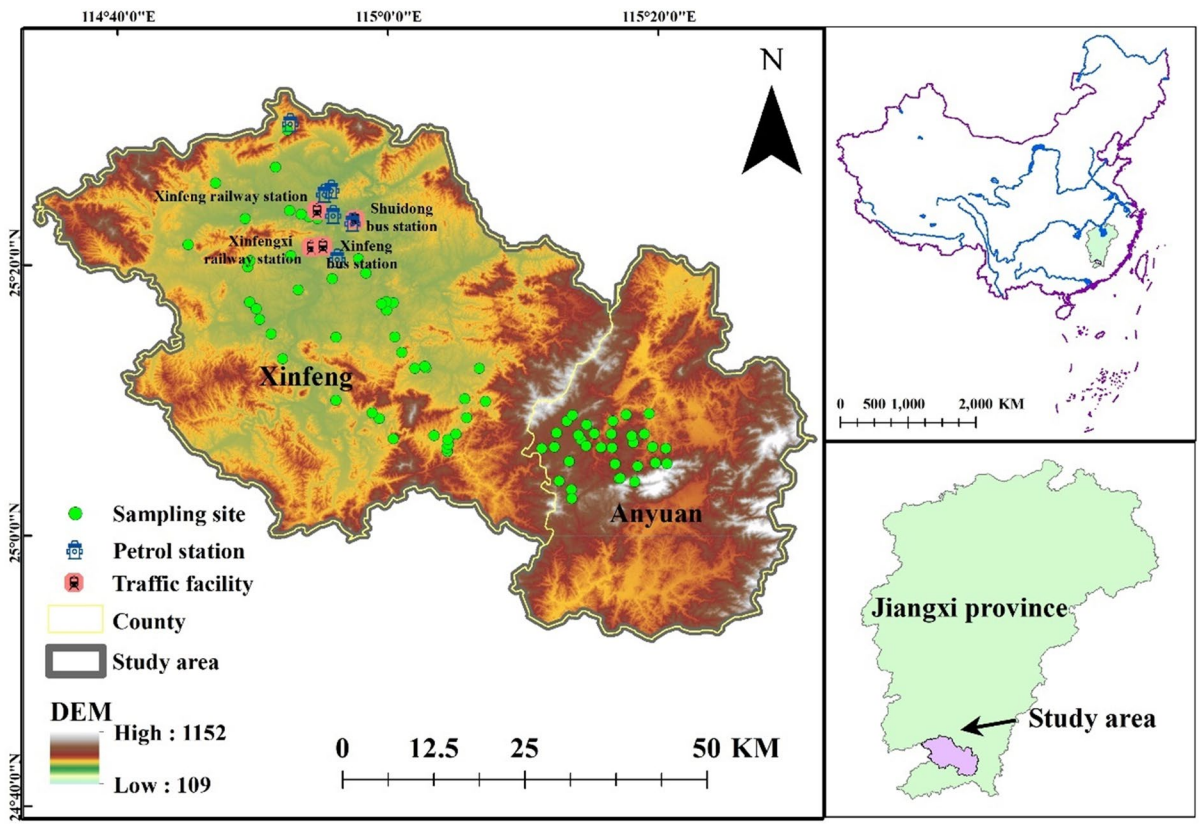

Fig. 1 Study area

bags in the cool space with no direct sunlight before transport to laboratory for further analysis. After small stones as well as organic debris removed and air-dried, the soil samples were broken up and sifted through the fine sieve of 1 mm. Then, the Hg concentration was measured by the analyzer named Lumex (RA915M) with the detection limit of 0.3 $ng \cdot g^{-1}$. The GBW07447 (GSS18) was chosen as the reference sample for quality control.

Self-organizing map

SOM belongs to unsupervised neural network, with which high-dimensional data is able to be projected to two-dimensional self-organizing network called "feature map" (Farsadnia et al., 2014; Li et al., 2018). Thanks to the good perform on classification and visualization, it has become an flexible and robust approach to detect the characteristics of the observing data (Melo et al., 2019; Tsuchihara et al., 2020). SOM consists of both input and output layers, and the *n*-dimensional input variables are stored in the input layer. Output layer neurons mapped from input variables have the nodes arranged in hexagonal lattice, of which the topology as well as numbers can be defined subjectively. Besides, the input as well as output neurons are connected by weight vectors, whose dimension is corresponding to the number of input variables (Rahman et al., 2022). The SOM training begins with weight initialization using random numbers, and the Euclidian distance between the input variable and weight for each output neuron is calculated. The distant neurons restrain each other while the neighboring ones stimulate each other during the SOM adjustment. The final winning neuron is seen as the best matching unit (BMU) of the input (Wang et al., 2020). The topographic error and quantization error are for the accuracy measurement of SOM. In this study, the 9×6 SOM was constructed for Hg concentration classification and visualization combined with k-means clusering, which was conducted in MATLAB 2012 using SOM Toolbox (http://www.cis.hut.fi/projects/somtoolbox/).

Geoaccumulation index

Geoaccumulation index performs well in evaluating pollution degree for the heavy metals in soil (Bing et al., 2011), which is calculated as:

$$I_{geo} = \log_2 \frac{C_{Hg}}{1.5BG_{Hg}} \quad (1)$$

where C_{Hg} denotes the Hg concentration, and BG_{Hg} is the background value of Hg in Jiangxi Province from Chinese Environmental Protection Administration (1990).

Potential ecological risk

The potential ecological risk index is adopted to evaluate the heavy metal pollutions as well as their toxicological effects (Wang et al., 2020). In this study, the *Er* of Hg can be calculated as:

$$\mathrm{Er} = \frac{\mathrm{TR}_c \cdot C_{Hg}}{\mathrm{BG}_{Hg}} \quad (2)$$

where TR_c denotes the toxic response coefficient (Hg = 40), and C_{Hg} as well as BG_{Hg} are the Hg concentration and its background value is as same as formula 1.

Positive matrix factorization

PMF, initially adopted for the source identification of particulate matter, has already become a classic approach for quantitative pollutant source apportionment (He et al., 2022). It is expressed as:

$$x_i = \sum_{k=1}^{p} u_{ik} \cdot v_k + \varepsilon_i \quad (3)$$

where x_i denotes the measured value for the *i*th sample, and p, u, v, ε are the number of factors, the profile for each source, the contribution to each sample from each factor and the residual of each sample, respectively. By minimizing the objective function Q, PMF obtains the factor contributions:

$$Q = \sum_{i=1}^{n} \left[\frac{x_i - \sum_{k=1}^{p} u_{ik} \cdot v_k}{\varepsilon_i} \right]^2 \quad (4)$$

Besides, the input uncertainty for each sample *i* is:

$$\mathrm{uu} = \sqrt{(E \times c)^2 + (0.5 \times M)^2} \; (c > M) \quad (5)$$

$$uu = \frac{5}{6}M\ (c \le M) \tag{6}$$

where c, E and M are the Hg concentration, error fraction of instrument and detection limit, respectively.

PMF 5.0 from US Environmental Protection Agency was adopted to quantify the contribution of pollution sources for Hg in this research.

Results and discussion

Summary Statistics for Hg concentration

The description for Hg concentration in the study area is shown in Table 1. It can be seen that the Hg concentration in Anyuan ranged in 1.4–345.6 μg kg^{-1} (n = 32) with the average of 41.1 μg kg^{-1}, which indicated that the distribution of mercury content was uneven particularly. This is supported by the high concentration variance (CV = 138.4%). Of note, one site showed Hg concentrations as high as 345.6 μg kg^{-1} Hg, over eight times the average of Anyuan and higher than Hg concentrations reported near coal-fired power plants (Song et al., 2021). By contrast, the Hg concentration ranged in 8.5–239.0 μg kg^{-1} (n = 46) in Xinfeng (Table 1), showing a lower variance than that of Anyuan, which could also be learned from Figure S1. The standard deviation (SD) and the coefficient of variation (CV (%)) of Xinfeng were also lower. Besides, the average Hg concentration of Xinfeng was 53.9 μg kg^{-1} (Table 1, Figure S1), which exceeded the mean mercury concentration of Anyuan. This indicated that the overall Hg content of the farmland planted with rice was higher than that of the farmland planted with fruit trees. The Hg average of Xinfeng also increased the average of the whole study region, which was 48.7 μg kg^{-1}. The averages of Hg concentration for Anyuan, Xinfeng and the whole study area were 0.49, 0.64 and 0.58 times of the background value in Jiangxi Province (84 μg kg^{-1} Hg), respectively (Table 1), which verified that the farming area near mining activities had no heavy mercury pollution on the whole (Chinese Environmental Protection Administration, 1990).

Spatial distribution of Hg concentration

The result of inverse distance weighting (IDW) interpolation for Hg concentration is shown in Fig. 2. It could be seen that there was no obvious Hg pollution in the most region of Anyuan except for the south region, where pollution level was close to the average (344 μg kg^{-1}) of certain reported typical pollution areas like the coal-fired power plants area in Heilongjiang (Li et al., 2017). According to on-the-spot investigation, there was farmland around polluted sites. Thus, the high Hg concentration probably caused by the solid wastes as well as the wastewater produced by farmland activities. Moreover, the excessive application of pesticides, organic manures and fertilizers could also contribute to soil mercury content (Cai et al., 2015; Feng et al., 2022; Zhong et al., 2016). The north region of Xinfeng also showed obvious Hg pollution, while most other areas of Xinfeng had relatively lower Hg concentration (Fig. 2). The sampling site with the highest Hg concentration in this region was near some railway stations, bus stations and petrol stations according to the online satellite map (https://map.baidu.com/@12959765,4842486,13z). As the important transportation hubs of Xinfeng, the railway stations and bus stations gathered passengers from various regions, who carried different motor vehicles. A large number of traffic vehicles, together with the running of trains, caused the mercury enrichment in nearby soil (Liu et al., 2012). The high soil mercury concentration was also discovered near the petrol stations and highway in the most north of Xinfeng on the basis of online map (Figs. 1 and 2), where large amount of vehicles gathered every day. The traffic discharged toxic tail gas into atmosphere continuously, and pollutants entered soil with falling dust (Lenka et al., 2017). The spatial distribution

Table 1 Statistical description for Hg concentrations (μg kg^{-1})

Area	n	Max	Min	Mean	SD	CV (%)
Anyuan	32	345.6	1.4	41.1	56.9	138.4
Xinfeng	46	239.0	8.5	53.9	39.5	73.2
Total	78	345.6	1.4	48.7	47.8	98.2

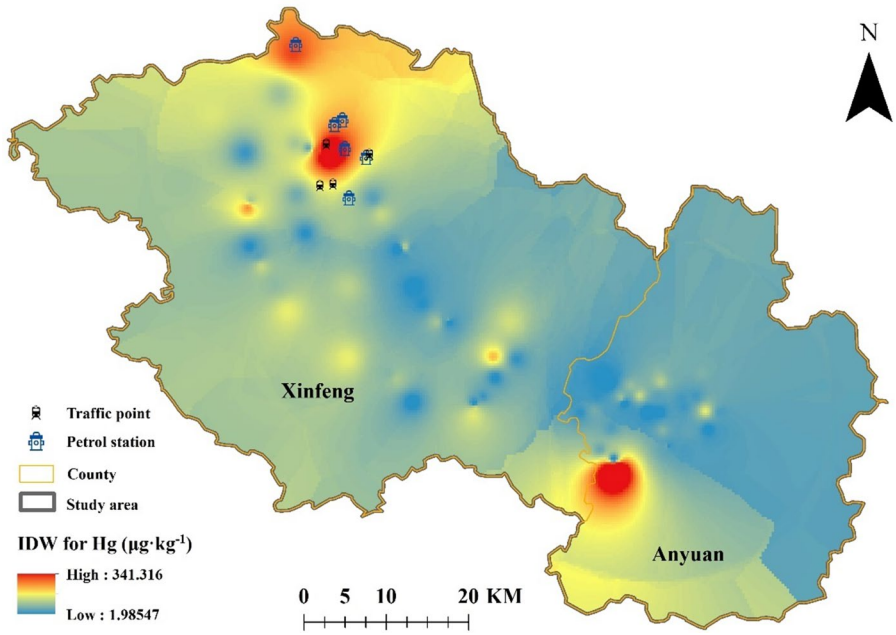

Fig. 2 Inverse distance weighted interpolation for Hg concentrations

analysis of Hg concentration showed that traffic pollution was the important pollution source for Hg in Xinfeng, while the inappropriate agricultural activities caused heavy mercury pollution in some areas of Anyuan. Besides, the Hg pollution in Anyuan was concentrated in the south, while that of Xinfeng was in the north.

Classification for Hg concentration using self-organizing map

A two-dimensional self-organizing map of Hg concentration (left) and a U-matrix of SOM (right) were constructed (Fig. 3a). The research also classified the samples into four clusters combined with k-means cluster algorithm according to their SOM result (Fig. 3b), and the sample positions in each cluster were identified in Fig. 3c. The topographic error and the quantization error for SOM were 0.590 and 3.374, respectively.

It could be learnt that most samples with low Hg concentration belonged to Cluster I (Fig. 3ab), which also evidenced that there was no Hg pollution in most study area (Fig. 3c). Many other samples were divided into Cluster II, which scattered throughout the whole rice field in Xinfeng (Fig. 3c), while Anyuan had barely soil samples belonged to this cluster. This spatially reflected that the mercury concentration in the rice fields of Xinfeng was slightly higher than that of the fruit fields in Anyuan as well as the background value of the whole Jiangxi Province (Chinese Environmental Protection Administration, 1990). It was probably because the artificial additions like Hg-containing pesticides facilitate mercury enrichment to a small extent (Yuan et al., 2021). The conversion to sustainable organic farming may avoid the deeper enrichment of mercury. The samples near petrol stations and highway in the most north part of Xinfeng was classified into Cluster III (Fig. 3c). The sample close to the railway stations in Xinfeng as well as the sample in the southwest of Anyuan belonged to Cluster IV (Fig. 3c), which reflected the significant contributions from traffic source and agricultural source (Hu et al., 2021; Shang et al., 2018; Wang et al., 2022). Hence, the traffic facility or farmland with Hg pollution was supposed to be given enough attention or even the relative treating measures. It could also be excavated that the agricultural source promoted minor increase of Hg content in the large scale of Xinfeng, while led to serious Hg enrichment in a small scale in the south of Anyuan.

A1-A32 and X1-X46 denote the samples in Anyuan and Xinfeng, respectively.

Fig. 3 Self-organic map and k-means cluster for Hg concentrations

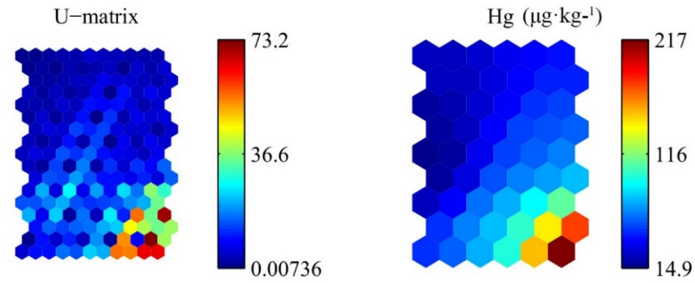

(a) Self-organic map for Hg concentrations

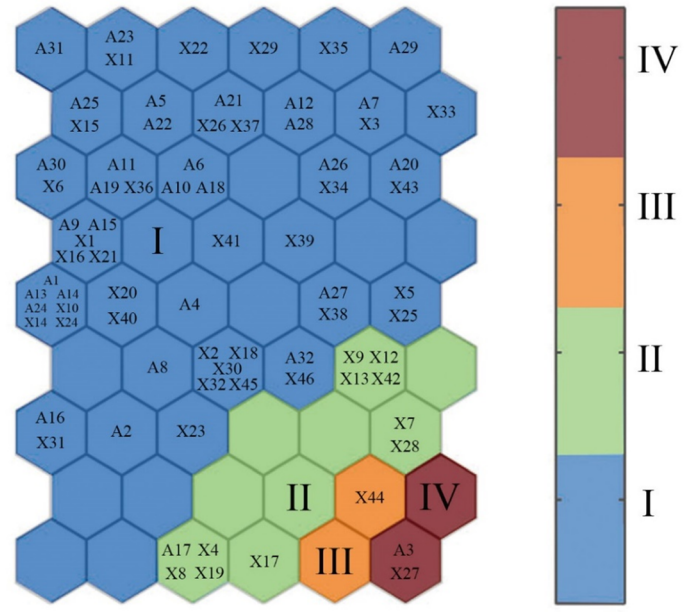

(b) K-means cluster for Hg concentrations

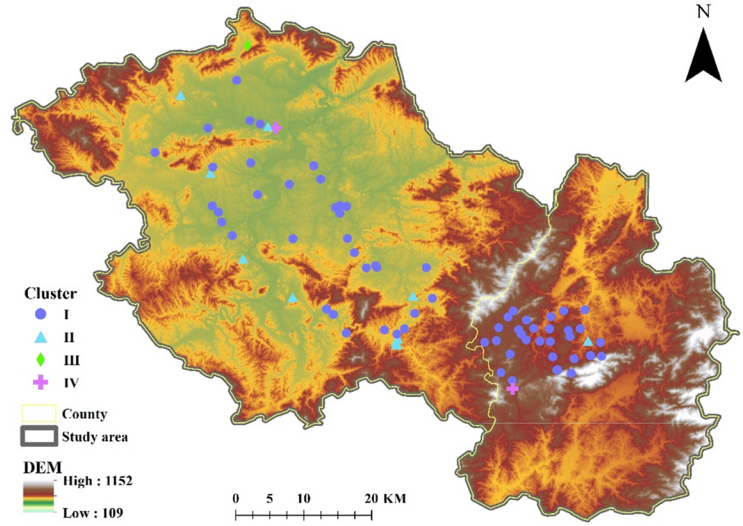

(c) Spatial distribution of Hg concentrations for each cluster

Assessment for Hg pollution risk

The geoaccumulation index for each sample and the interpolation of it is shown in Fig. 4, and the correspondence between I_{geo} and pollution degree is in Table S1. Most samples and their nearby areas had negative I_{geo} due to the low Hg concentration. There was no high I_{geo} near rare earth mining and smelting activities, which indicated that mining and smelting rarely caused mercury pollution to surrounding areas. The rice planting had no local pollution as well. Besides, the individual sampling points with the I_{geo} between 0 and 1 (blue circle) were at the pollution degree of "No pollution ~ Moderate pollution" (Table S1). The two blue circles of this category at the north part of Xinfeng (Fig. 4) were at the sides of petrol stations and railway stations, thus the traffic source significantly contributed to their pollution degree. However, the mercury-containing compounds in vehicle fuels such as oil, coal and minerals were volatilized into air in the combustion process and made the air contain mercury vapor as well as dust containing mercury compounds. Moreover, mercury further settled in the surrounding soil with the release of tail gas (Debnárová & Weissmannová, 2010; Yaylalı-Abanuz, 2011). Besides, the highest I_{geo} marked with red circle appeared in farmland in the southwest of Anyan, which belonged to the moderate pollution. As reported that the use of mercury-containing pesticides and fertilizers would increase the soil mercury concentration and cause soil pollution (Dong et al., 2017), thus the locally artificial addition was very likely the primary reason leading to this risk. By contrast, the same level pollution did not exist in the vast area of Xinfeng. The absence of Hg pollution in the most farmlands of the research region may be due to the restrictions on the production and usage of the mercury-containing pesticides in recent decades.

The potential ecological risk index of Hg for Xinfeng and Anyuan and the corresponding interpolation result is in Fig. 5, and the relative criteria for ecological risk degrees are in Table S2. Most samples in both Anyuan and Xinfeng had the *Er* lower than 40, which indicated the low potential ecological risk in the areas near these sampling positions (Fig. 5). The yellow circles had the *Er* between 40 and 80, which reflected the moderate ecological risks in the central and north areas of the study region. These areas of moderate ecological risk were near the petrol stations, railway stations and highway in Xinfeng, which meant that the traffic pollution not only threatened human health through air pollution, but also promoted soil Hg enrichment and caused ecological risk as well as human health risk indirectly (Li & Tse, 2015). Moreover, the sampling site marked with orange circle had the considerable ecological risk, which was also near the railway stations. In contrast, neither the

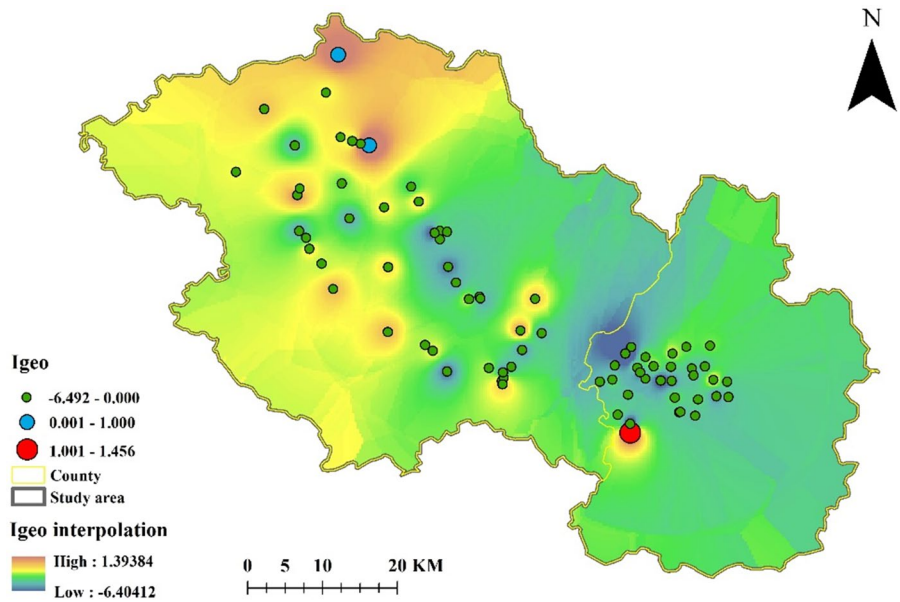

Fig. 4 I_{geo} and IDW interpolation for I_{geo}

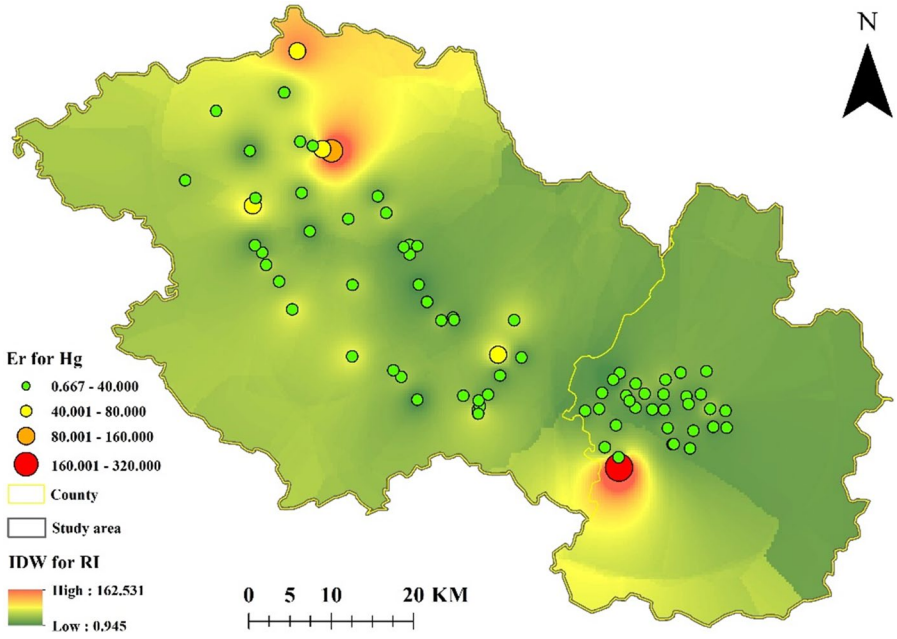

Fig. 5 *Er* and IDW interpolation for *Er*

low ecological risk nor the moderate ecological risk appeared in Anyuan. Therefore, it must be noted that the sampling position in the southwest farmland of Anyuan marked with red circle had the high ecological risk ($160 \leq Er < 320$). This local serious pollution may be caused by excessive pesticide additions, and it would bring about high human health risk (Raj et al., 2017; Tutton et al., 2022). The mercury enriched in the plants when its content was too high, which had a toxic effect on plants. It affected the absorption of nutrients by the plant roots, and then impacted the growth of their aboveground parts. It would also damage the human function when it entered human body through food chains (Jiang et al., 2021; Yeganeh et al., 2013). Thus, the local mercury pollution should be managed targetedly in Anyuan. On the contray, Xinfeng had no so serious pollution risk in the rice field.

Pollution source identification for Hg

The uncertainty result (Figure S2) for the input of PMF model was calculated (Fig. 6) according to formula 5 since the concentrations of all mercury samples were above the detection limit. The predetermined number for the explanatory factors was 3 in PMF. The Q_{robust} was approach to Q_{true} after ten runs of the PMF calculation using the Hg concentration

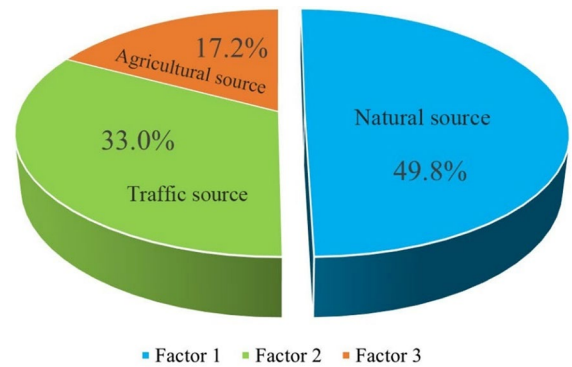

Fig. 6 Factor contribution according to positive matrix factorization

data and uncertainty file, which acquired an $R^2 > 0.9$. These results suggested that PMF had good performance for quantifying the explanatory factors.

In term of PMF result (Fig. 6), factor 1 had the largest contribution (49.8%) to Hg pollution. It could be learnt that most samples with lower Hg concentrations had negative I_{geo} and lower potential ecological risk indexes. The main sources of the soil Hg contents in most area of the research region were originally from the soil parent material, rock weathering and other natural sources (Carvalho et al., 2019; Nezhad et al., 2014; Rodríguez Martín et al., 2013).

Therefore, the factor 1 with the contribution of 49.8% was most likely the natural sources.

Combined with the analysis of spatial distribution of Hg concentration as well as the ecological risk assessment for Hg pollution, most samples with higher geoaccumulation indexes and higher potential ecological risk indexes were close to highway or transportation facilities such as railway station and petrol station. Ganzhou City has been the important transportation hub in the southeast of China, which connects four provinces including Fujian, Jiangxi, Guangdong and Hunan (Cheng, 2009). Roads and other traffic facilities were under great pressure from traffic, which made large amount of harmful gas in the automobile exhaust discharged into the air continuously, and polluted surrounding soil at a certain degree. Therefore, it was concluded that factor 2 with the contribution of 33% was the traffic source, which was the large pollution source. In the face of serious dust pollution near roads, railway stations and petrol stations, it is suggested to build more green belts with strong adsorption capacity to gradually reduce air and soil pollution, decrease ecological risk and improve the quality of ecological environment (Gupta et al., 2016; Islam et al., 2012; Jiang et al., 2020).

Factor 3 contributed 17.2% calculated by PMF, which was the factor that contributed the least to mercury pollution. Except for traffic pollution, there was also local Hg pollution risk in farmland due to the inappropriate agricultural additions. Excessive use of pesticide and fertilizer had caused mercury enrichment in the soil. The cumulative Hg entered the human body and other organisms through the food chains, which caused serious consequences to human health and the whole ecosystem because of the highly toxic of mercury (Liu et al., 2021; Ma et al., 2017; Mahbub et al., 2017). The agricultural pollution had the smaller scale compared with the traffic pollution, which may be attribute to the excessive use of pesticides by individuals. Besides, Hg pollution was not detected in many other farmlands, especially the rice field in Xinfeng. It could be concluded that there was no excessive addition of mercury-containing substances that caused heavy Hg pollution at the large scale. Thus, factor 3 was possibly the agricultural pollution source.

Conclusions

This research investigated the spatial heterogeneity, clustering characteristics, ecological risks as well as pollution source contributions for Hg in a typical area. Results showed that there was no large-scale and heavy mercury pollution near mining or smelting areas of rare earth. However, some areas near railway stations, petrol stations and highway in Xinfeng had high Hg concentrations, and high Hg enrichment also appeared in farmland in the southwest of Anyuan according to spatial analysis and SOM. It reflected the serious impact on local soil environment from heavy traffic and inappropriate agricultural additions. The SOM classification also indicated that most samples in the rice field of Xinfeng had a slight increase of mercury compared with the most field of Anyuan, but this had not caused obvious pollution.

Besides, the geoaccumulation index distribution displayed that mercury from automobile exhaust emission entered the soil, causing certain pollution accumulation in the soil near highways, railway stations and gas stations in Xinfeng. The nearby potential ecological risk had increased as well. In contrast, the sampling position in the farmland in Anyuan had moderate pollution measured by I_{geo} and high ecological risk measured by Er. The enriched Hg harmed both human and ecological health, which was supposed to be given targeted pollution treatment. In addition, it could be concluded that the natural source like parent material and rock weathering was the factor with the largest contribution of the soil Hg contents. The traffic source causing different pollution degrees and health risks was factor 2 because of the larger-scale pollution than that of agricultural source. The agricultural pollution source appeared in Anyuan at a small scale was factor 3 in this typical area. This research gives good comprehension of Hg pollution in the rare earth mining area with developed traffic and agriculture and will provide scientific evidence for targeted Hg pollution treatment.

Author Contributions ZF was involved in methodology, modeling, software, writing—original draft. LD helped in data curation, visualization, reviewing and software. YG contributed to resources, data curation and validation. GG was involved in resources, validation and investigation. LW helped in conceptualization, resources, reviewing and supervision. GZ contributed to resources, software, and reviewing. YH was involved in

resources, investigation and reviewing. TL helped in resources, reviewing and supervision.

Funding This research was supported by the Qinghai Province Key Research and Development and Transformation Program (2023-QY-205) and Jiangxi Province Key Research and Development Project (20212BBG73017).

Data availability The data that support the findings of this study is available from the corresponding author upon reasonable request.

Declarations

Conflict of interest The authors declare no competing interests.

Informed consent Informed consent was obtained from all individual participants included in the study.

Consent for publication Consent to publish has been received from all participants.

References

Administration, C. E. P. (1990). *Elemental background values of soils in China*. Environmental Science Press of China.

Antoniadis, V., Shaheen, S. M., Levizou, E., Shahid, M., Niazi, N. K., Vithanage, M., Ok, Y. S., Bolan, N., & Rinklebe, J. (2019). A critical prospective analysis of the potential toxicity of trace element regulation limits in soils worldwide: Are they protective concerning health risk assessment?-A review. *Environment International, 127*, 819–847.

Beckers, F., Awad, Y. M., Beiyuan, J., Abrigata, J., Mothes, S., Tsang, D. C., & Rinklebe, J. (2019). Impact of biochar on mobilization, methylation, and ethylation of mercury under dynamic redox conditions in a contaminated floodplain soil. *Environment International, 127*, 276–290.

Bing, H., Wu, Y., Sun, Z., & Yao, S. (2011). Historical trends of heavy metal contamination and their sources in lacustrine sediment from Xijiu Lake, Taihu Lake Catchment, China. *Journal of Environmental Sciences, 23*(10), 1671–1678.

Cai, L., Xu, Z., Bao, P., He, M., Dou, L., Chen, L., Zhou, Y., & Zhu, Y. (2015). Multivariate and geostatistical analyses of the spatial distribution and source of arsenic and heavy metals in the agricultural soils in Shunde, Southeast China. *Journal of Geochemical Exploration, 148*, 189–195.

Campos, J. A., Esbrí, J. M., Madrid, M. M., Naharro, R., Peco, J., García-Noguero, E. M., & Higueras, P. (2018). Does mercury presence in soils promote their microbial activity? The Almadenejos case (Almadén mercury mining district, Spain). *Chemosphere, 201*, 799–806.

Carvalho, G. S., Oliveira, J. R., Curi, N., Schulze, D. G., & Marques, J. J. (2019). Selenium and mercury in Brazilian Cerrado soils and their relationships with physical and chemical soil characteristics. *Chemosphere, 218*, 412–415.

Chary, N. S., Kamala, C. T., & Raj, D. S. S. (2008). Assessing risk of heavy metals from consuming food grown on sewage irrigated soils and food chain transfer. *Ecotoxicology and Environmental Safety, 69*(3), 513–524.

Cheng, D. (2009). Development path for small towns in underdeveloped areas-a case of Ganzhou City in Jiangxi Province. *Asian Agricultural Research, 1*(1812-2016–142814), 10–15.

Debnárová, A., & Weissmannová, H. (2010). Assessment of heavy metal pollution (Cd, Cu, Pb, Hg) in urban soils of roadsides in Brno. *Trans Transp Sci, 3*(4), 147–156.

Dong, H., Lin, Z., Wan, X., & Feng, L. (2017). Risk assessment for the mercury polluted site near a pesticide plant in Changsha, Hunan, China. *Chemosphere, 169*, 333–341.

Farsadnia, F., Kamrood, M. R., Nia, A. M., Modarres, R., & Sadatinejad, J. (2014). Identification of homogeneous regions for regionalization of watersheds by two-level self-organizing feature maps. *Journal of Hydrology, 509*(4), 387–397.

Feng, Z., Xu, C., Zuo, Y., Luo, X., Wang, L., Chen, H., Xie, X., Yan, D., & Liang, T. (2022). Analysis of water quality indexes and their relationships with vegetation using self-organizing map and geographically and temporally weighted regression. *Environmental Research, 216*, 114587.

Gupta, G. P., Kumar, B., & Kulshrestha, U. C. (2016). Impact and pollution indices of urban dust on selected plant species for green belt development: Mitigation of the air pollution in NCR Delhi, India. *Arabian Journal of Geosciences, 9*(2), 1–15.

He, H., Wei, H., Wang, Y., Wang, L., Qin, Z., Li, Q., Shan, F., Fan, Q., & Du, Y. (2022). Geochemical and statistical analyses of trace elements in lake sediments from Qaidam Basin, Qinghai-Tibet Plateau: Distribution characteristics and source apportionment. *International Journal of Environmental Research and Public Health, 19*, 2341.

Hu, H., Han, L., Li, L., Wang, H., & Xu, T. (2021). Soil heavy metal pollution source analysis based on the land use type in Fengdong District of Xi'an, China. *Environmental Monitoring and Assessment, 193*(10), 1–14.

Islam, M. N., Rahman, K. S., Bahar, M. M., Habib, M. A., Ando, K., & Hattori, N. (2012). Pollution attenuation by roadside greenbelt in and around urban areas. *Urban Forestry & Urban Greening, 11*(4), 460–464.

Jiang, H., Cai, L., Hu, G., Wen, H., Luo, J., Xu, H., & Chen, L. (2021). An integrated exploration on health risk assessment quantification of potentially hazardous elements in soils from the perspective of sources. *Ecotoxicology and Environmental Safety, 208*, 111489.

Jiang, H., Cai, L., Wen, H., Hu, G., Chen, L., & Luo, J. (2020). An integrated approach to quantifying ecological and human health risks from different sources of soil heavy metals. *Science of the Total Environment, 701*, 134466.

Lawrence, D. J., Feldman, W. C., Goldsten, J. O., Maurice, S., Peplowski, P. N., Anderson, B. J., Bazell, D., McNutt, R. L., Nittler, L. R., Prettyman, T. H., Rodgers, D. J., Solomon, S. C., & Weider, S. Z. (2013). Evidence for water ice near Mercury's north pole from MESSENGER Neutron

Spectrometer measurements. *Science, 339*(6117), 292–296. https://doi.org/10.1126/science.1229953

Lenka, D., Beáta, B., Jozef, O., Július, Á., & Tomáš, L. (2017). Assessment of air pollution by toxic elements on petrol stations using moss and lichen bag technique. *Plant, Soil and Environment, 63*(8), 355–361.

Li, H., Xu, F., & Li, Q. (2020). Remote sensing monitoring of land damage and restoration in rare earth mining areas in 6 counties in southern Jiangxi based on multisource sequential images. *Journal of Environmental Management, 267*, 110653.

Li, R., Wu, H., Ding, J., Fu, W., Gan, L., & Li, Y. (2017). Mercury pollution in vegetables, grains and soils from areas surrounding coal-fired power plants. *Scientific Reports, 7*(1), 1–9.

Li, T., Sun, G., Yang, C., Liang, K., Ma, S., & Huang, L. (2018). Using self-organizing map for coastal water quality classification: Towards a better understanding of patterns and processes. *The Science of the Total Environment, 628–629*, 1446–1459.

Li, W. C., & Tse, H. F. (2015). Health risk and significance of mercury in the environment. *Environmental Science and Pollution Research, 22*(1), 192–201.

Liu, Q., Liu, Y., & Zhang, M. (2012). Mercury and cadmium contamination in traffic soil of Beijing, China. *Bulletin of Environmental Contamination and Toxicology, 2*, 154–157.

Liu, S., Wang, X., Guo, G., & Yan, Z. (2021). Status and environmental management of soil mercury pollution in China: A review. *Journal of Environmental Management, 277*, 111442.

Lv, J. (2019). Multivariate receptor models and robust geostatistics to estimate source apportionment of heavy metals in soils. *Environmental Pollution, 244*, 72–83.

Ma, Z., Wang, Q., Zhang, Z., & Zhou, X. (2017). Mercury distribution along the food chain of a wetland ecosystem at Sanjiang Plain, Northeast China. *Bulletin of Environmental Contamination and Toxicology, 98*(2), 162–166.

Magesh, N. S., Tiwari, A., Botsa, S. M., & da Lima Leitao, T. (2021). Hazardous heavy metals in the pristine lacustrine systems of Antarctica: Insights from PMF model and ERA techniques. *Journal of Hazardous Materials, 412*, 125263.

Mahbub, K. R., Krishnan, K., Naidu, R., Andrews, S., & Megharaj, M. (2017). Mercury toxicity to terrestrial biota. *Ecological Indicators, 74*, 451–462.

Mari, M., Nadal, M., Schuhmacher, M., & Domingo, J. L. (2010). Application of self-organizing maps for PCDD/F pattern recognition of environmental and biological samples to evaluate the impact of a hazardous waste incinerator. *Environmental Science & Technology, 44*(8), 3162–3168.

Melo, D. S., Gontijo, E. S., Frascareli, D., Simonetti, V. C., Machado, L. S., Barth, J. A., Moschini-Carlos, V., Pompêo, M. L., Rosa, A. H., & Friese, K. (2019). Self-organizing maps for evaluation of biogeochemical processes and temporal variations in water quality of subtropical reservoirs. *Water Resources Research, 55*(12), 10268–10281.

Nezhad, M. T. K., Mohammadi, K., Gholami, A., Hani, A., & Shariati, M. S. (2014). Cadmium and mercury in topsoils of Babagorogor watershed, western Iran: Distribution, relationship with soil characteristics and multivariate analysis of contamination sources. *Geoderma, 219*, 177–185.

Osterwalder, S., Huang, J. H., Shetaya, W. H., Agnan, Y., Frossard, A., Frey, B., Alewell, C., Kretzschmar, R., Biester, H., & Obrist, D. (2019). Mercury emission from industrially contaminated soils in relation to chemical, microbial, and meteorological factors. *Environmental Pollution, 250*, 944–952.

Rahman, A. S., Kono, Y., & Hosono, T. (2022). Self-organizing map improves understanding on the hydrochemical processes in aquifer systems. *Science of the Total Environment, 846*, 157281.

Raj, D., Chowdhury, A., & Maiti, S. K. (2017). Ecological risk assessment of mercury and other heavy metals in soils of coal mining area: A case study from the eastern part of a Jharia coal field, India. *Human and Ecological Risk Assessment: An International Journal, 23*(4), 767–787.

Rodríguez Martín, J. A., Carbonell, G., Nanos, N., & Gutiérrez, C. (2013). Source identification of soil mercury in the Spanish Islands. *Archives of Environmental Contamination and Toxicology, 64*(2), 171–179.

Shahid, M., Khalid, S., Bibi, I., Bundschuh, J., Niazi, N. K., & Dumat, C. (2020). A critical review of mercury speciation, bioavailability, toxicity and detoxification in soil-plant environment: Ecotoxicology and health risk assessment. *Science of the Total Environment, 711*, 134749.

Shang, E., Xu, E., Zhang, H., & Huang, C. (2018). Spatial-temporal trends and pollution source analysis for heavy metal contamination of cultivated soils in five major grain producing regions of China. *Environmental Science, 39*(10), 4670–4683.

Song, Z., Wang, C., Ding, L., Chen, M., Hu, Y., Li, P., & Feng, X. (2021). Soil mercury pollution caused by typical anthropogenic sources in China: Evidence from stable mercury isotope measurement and receptor model analysis. *Journal of Cleaner Production, 288*, 125687.

Tabassum, R. A., Shahid, M., Dumat, C., Niazi, N. K., Khalid, S., Shah, N. S., Imran, M., & Khalid, S. (2019). Health risk assessment of drinking arsenic-containing groundwater in Hasilpur, Pakistan: Effect of sampling area, depth, and source. *Environmental Science and Pollution Research, 26*(20), 20018–20029.

Taghvaee, S., Sowlat, M. H., Mousavi, A., Hassanvand, M. S., Yunesian, M., Naddafi, K., & Sioutas, C. (2018). Source apportionment of ambient PM2. 5 in two locations in central Tehran using the Positive Matrix Factorization (PMF) model. *Science of the Total Environment, 628*, 672–686.

Tang, Z., Fan, F., Deng, S., & Wang, D. (2020). Mercury in rice paddy fields and how does some agricultural activities affect the translocation and transformation of mercury-A critical review. *Ecotoxicology and Environmental Safety, 202*, 110950.

Tsuchihara, T., Shirahata, K., Ishida, S., & Yoshimoto, S. (2020). Application of a Self-organizing map of isotopic and chemical data for the identification of groundwater recharge sources in Nasunogahara Alluvial Fan, Japan. *Water, 12*, 278. https://doi.org/10.3390/w12010278

Tutton, C., Young, S., & Habib, K. (2022). Pre-processing of e-waste in Canada: Case of a facility responding to changing material composition, Resources. *Environment and Sustainability, 9*, 100069.

Wang, X., Sun, Y., Guo, H., & Wang, H. (2022). Analysis of soil heavy metal hg pollution source based on geodetector. *Polish Journal of Environmental Studies, 31*(1), 347–355.

Wang, Y., Yang, Y., Liu, X., Zhao, J., Liu, R., & Xing, B. (2021). Interaction of microplastics with antibiotics in aquatic environment: Distribution, adsorption and toxicity. *Environmental Science & Technology, 55*(23), 15579–15595.

Wang, Z., Xiao, J., Wang, L., Liang, T., & Rinklebe, J. (2020). Elucidating the differentiation of soil heavy metals under different land uses with geographically weighted regression and self-organizing map. *Environmental Pollution, 260*, 114065.

WHO. (2019). Mercury and health. World Health Organization. Accessed on September 16, 2019: https://www.who.int/news-room/fact-sheets/detail/mercury-and-health.

Xue, J., Jiang, W., Gong, S., Fan, Y., & Li, X. (2013). An evaluation of heavy metals contamination in soils from Ganzhou navel orange orchards by geoaccumulation indexes and statistical analysis. *Chemistry and Ecology, 29*(7), 586–594.

Yang, X. J., Lin, A., Li, X. L., Wu, Y., Zhou, W., & Chen, Z. (2013). China's ion-adsorption rare earth resources, mining consequences and preservation. *Environmental Development, 8*, 131–136.

Yaylalı-Abanuz, G. (2011). Heavy metal contamination of surface soil around Gebze industrial area, Turkey. *Microchemical Journal, 99*(1), 82–92.

Yeganeh, M., Afyuni, M., Khoshgoftarmanesh, A. H., Khodakarami, L., Amini, M., Soffyanian, A. R., & Schulin, R. (2013). Mapping of human health risks arising from soil nickel and mercury contamination. *Journal of Hazardous Materials, 244*, 225–239.

Yu, S., Wang, L., Zhao, J., & Shi, Z. (2020). Using structural equation modelling to identify regional socio-economic driving forces of soil erosion: A case study of Jiangxi province, southern China. *Journal of Environmental Management, 279*, 111616.

Yuan, X., Xue, N., & Han, Z. (2021). A meta-analysis of heavy metals pollution in farmland and urban soils in China over the past 20 years. *Journal of Environmental Sciences, 101*, 217–226.

Zhao, C., Shi, X., Xie, S., Liu, W., He, E., Tang, Y., et al. (2019). Ecological risk assessment of neodymium and yttrium on rare earth element mine sites in Ganzhou, China. *Bulletin of Environmental Contamination and Toxicology, 103*(4), 565–570.

Zhong, T., Chen, D., & Zhang, X. (2016). Identification of potential sources of mercury (Hg) in farmland soil using a decision tree method in China. *International Journal of Environmental Research and Public Health, 13*(11), 1111.

Zhou, Y., Aamir, M., Liu, K., Yang, F., & Liu, W. (2018). Status of mercury accumulation in agricultural soil across China: Spatial distribution, temporal trend, influencing factor and risk assessment. *Environmental Pollution, 240*, 116–124.

Publisher's Note Springer Nature remains neutral with regard to jurisdictional claims in published maps and institutional affiliations.